FEBS Letters 499 (2001) 182–186 FEBS 24971

Chemical shift mapping of shikimate-3-phosphate binding to the isolated N-terminal domain of 5-enolpyruvylshikimate-3-phosphate synthase

Melissa E. Stauffer[a,1], John K. Young[a,1], Gregory L. Helms[b], Jeremy N.S. Evans[a,b,*]

[a] *School of Molecular Biosciences, Washington State University, Pullman, WA 99164-4660, USA*
[b] *Center for NMR Spectroscopy, Washington State University, Pullman, WA 99164-4660, USA*

Received 9 April 2001; revised 9 May 2001; accepted 10 May 2001

First published online 1 June 2001

Edited by Thomas L. James

Abstract To facilitate evaluation of enzyme–ligand complexes in solution, we have isolated the 26-kDa N-terminal domain of 5-enolpyruvylshikimate-3-phosphate (EPSP) synthase for analysis by NMR spectroscopy. The isolated domain is capable of binding the substrate shikimate-3-phosphate (S3P), and this letter reports the localization of the S3P binding site using chemical shift mapping. Based on the NMR data, we propose that Ser23, Arg27, Ser197, and Tyr200 are directly involved in S3P binding. We also describe changes in the observed nuclear Overhauser effects (NOEs) that are consistent with a partial conformational change in the N-terminal domain upon S3P binding.

Key words: Chemical shift mapping; EPSP synthase; NMR; Secondary structure

1. Introduction

5-Enolpyruvylshikimate-3-phosphate (EPSP) synthase (EC 2.5.1.19) catalyzes the formation of EPSP (Fig. 1) from shikimate-3-phosphate (S3P) and phosphoenolpyruvate, a key step in the aromatic amino acid biosynthetic pathway of plants and bacteria. The enzyme is a promising target for antimicrobial [1], antiparasitic [2] and herbicide [3] development, since the pathway in which it occurs is absent from mammals. EPSP synthase is also the site of action of glyphosate (GLP), the active ingredient of the well-known herbicides RoundUp™ [4] and Touchdown™, and as such represents a model system for rational inhibitor design.

The crystal structure of unliganded EPSP synthase has been determined at 3.0 Å resolution by Stallings et al. [5]. It reveals a bilobal globular protein structure whose domains consist of repeated folding motifs ordered in a near-symmetric fashion (Fig. 1). The domains maintain an open conformation in the absence of substrates, but catalysis requires a conformational change to a closed state, and the particular substrate interactions that trigger this event are in question due to the presence of contradictory crystal structures in the literature. In 1997, Stallings et al. released several pictures of their enzyme·S3P complex [6], in which the enzyme maintains an open conformation, and all contacts between S3P and the enzyme are in the N-terminal domain. More recently, Schönbrunn et al. [7] have crystallized the binary enzyme•S3P complex in a closed conformation where S3P has multiple contacts with residues in both domains. Both structures have experimental caveats. The Stallings structure crystals were obtained by soaking preformed unliganded enzyme crystals in a solution of S3P, which may have biased the structure toward an open conformation. The Schönbrunn structure, on the other hand, was crystallized in the presence of formate and phosphate ions, which mimic the functional groups of GLP and may have induced the conformational change to the closed state. The conflict between these two structures can be resolved by examination of the liganded structure(s) of the enzyme in solution.

NMR spectroscopy has a unique ability to define the liganded solution state structure(s) of EPSP synthase with respect to the relative dynamics of the two domains and their subdomains, as well as the timescale of conformational changes that occur during the catalytic cycle. To facilitate analysis by NMR, we have prepared separate constructs encoding each of the two domains of EPSP synthase. Following NMR assignment of the 26-kDa N-terminal domain [8] and the discovery and characterization of its binding to S3P [9], we proceeded to obtain NMR assignments of the S3P-bound N-terminal domain. Here we report chemical shift changes that occur within the N-terminal domain upon S3P binding and map them to a proposed binding site based on their localization. We also describe some differences in the nuclear Overhauser effect (NOE) patterns of the free and bound domains that are consistent with a partial conformational change upon S3P binding. Because domain closure is not a possibility for this construct, the conformational changes due to S3P binding can be differentiated from those caused by (or resulting from) domain closure, which may ultimately aid the design of specific inhibitors of domain closure.

2. Materials and methods

2.1. Sample preparation

The N-terminal domain of EPSP synthase was produced [9] and NMR samples prepared [8] as described previously. Samples typically consisted of ~1 mM protein in 50 mM Tris, pH 7.8, 3 mM NaN_3, 1 mM DTT. In samples containing substrate, S3P was added from a concentrated stock to a final molar ratio of 1.5:1 (S3P:protein). S3P

*Corresponding author. Fax: (1)-509-335 9688.
E-mail: evansj@wsu.edu

[1] These authors contributed equally to this work.

Abbreviations: CSI, chemical shift index; EPSP, 5-enolpyruvylshikimate-3-phosphate; GLP, glyphosate; NOE, nuclear Overhauser effect; S3P, shikimate-3-phosphate

0014-5793/01/$20.00
PII: S0014-5793(01)02555-8

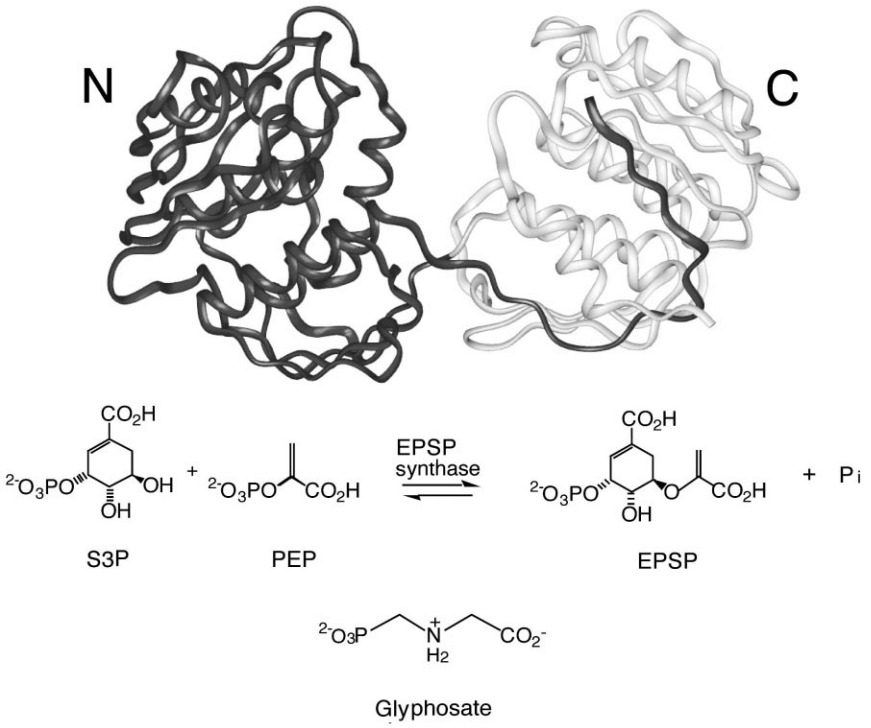

Fig. 1. Ribbon diagram of EPSP synthase showing how the protein was segmented into its constituent domains (PDB file 1EPS). 'N' and 'C' indicate the N-terminal and C-terminal domains, respectively. The reaction catalyzed by EPSP synthase is also shown, along with the structure of the inhibitor GLP.

binding was confirmed by observing the peak positions in the ^{15}N-heteronuclear single quantum coherence (HSQC) spectrum.

2.2. NMR spectroscopy

Sequential assignments and secondary structure prediction of the S3P-bound N-terminal domain were obtained as described for the domain alone [8]. The chemical shift list has been deposited in the BioMagResBank (http://www.bmrb.wisc.edu) under accession number 4848. NMR experiments were carried out at 22°C on a Varian Inova 500 NMR spectrometer (499.86 MHz, ^{1}H). The necessary correlation experiments were provided with Varian's Protein Pack software. Sequential backbone assignments of $^{1}H^{N}$ and ^{15}N nuclei were used to determine the extent of chemical shift changes upon S3P binding.

3. Results

3.1. Chemical shift mapping

From the individual assignments for the N-terminal domain alone and in the presence of S3P, we were able to extract a set of residues whose ^{1}H and ^{15}N chemical shifts changed the most upon S3P binding. This type of chemical shift mapping is often used to describe protein–protein and protein–ligand

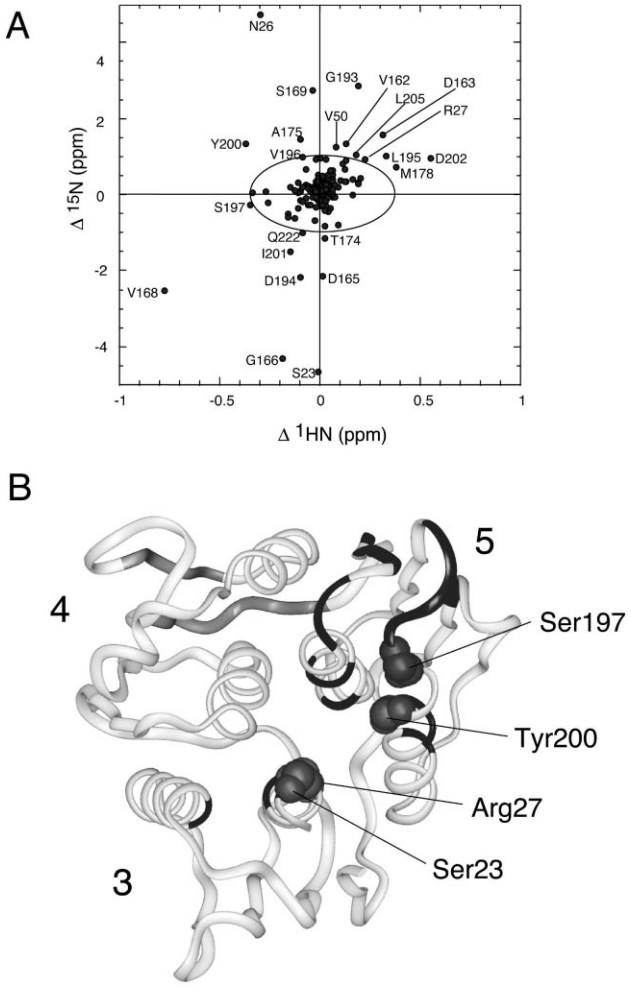

Fig. 2. A: Two-dimensional plot of the $^{1}H^{N}$ and ^{15}N chemical shift differences between the N-terminal domain alone and in the presence of S3P. The elliptical cutoff was defined as ±1 ppm for ^{15}N and ±0.35 ppm for $^{1}H^{N}$. Residues lying outside this cutoff were determined to be significantly shifted by S3P binding. B: Ribbon diagram of the N-terminal domain looking down the intersubdomain axis. Each subdomain is numbered according to Stallings et al. [5] and can be distinguished by its pair of helices. Residues in black experience significant changes in chemical shift upon S3P binding. Proposed S3P binding residues are rendered in CPK and are labeled. The charcoal segments in subdomain 4 undergo changes in their NOE patterns upon binding as described in the text.

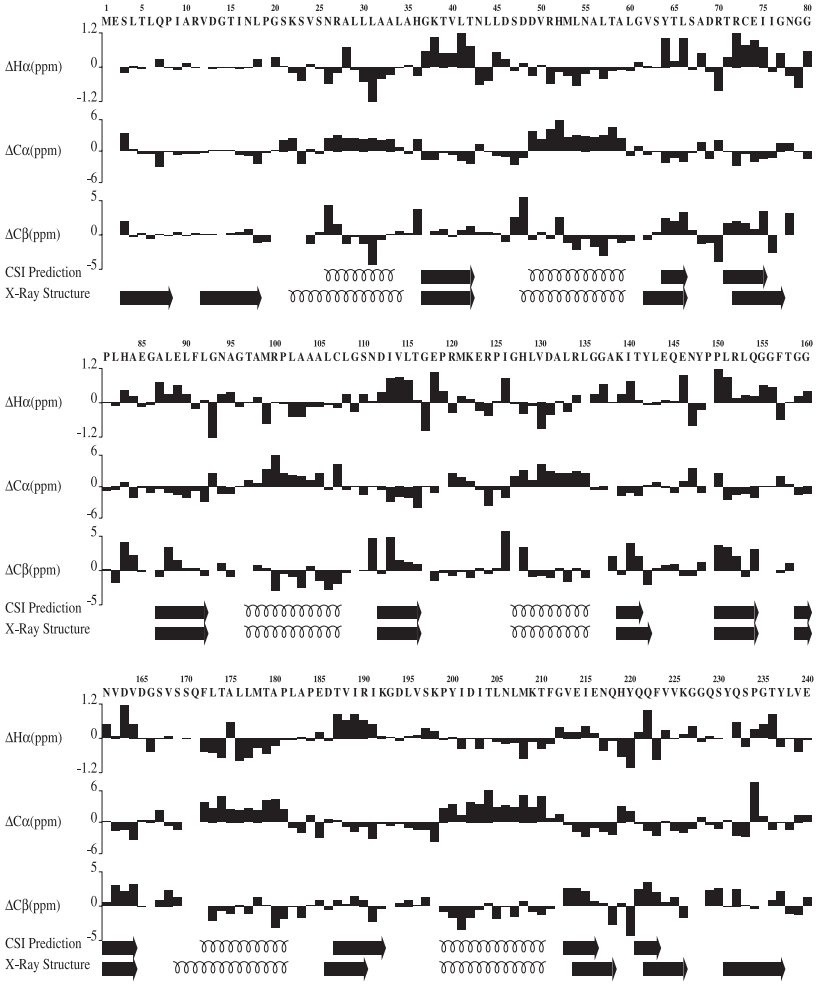

Fig. 3. Plots of the chemical shift index for $^{1}H^{\alpha}$, $^{13}C^{\alpha}$, and $^{13}C^{\beta}$ resonances of the N-terminal domain in the presence of S3P. The secondary structure prediction of these chemical shift changes is shown and compared with the secondary structure of the N-terminal domain within the full-length EPSP synthase as determined by X-ray crystallography [5].

interactions (see, for example, [10,11]), where an interface or binding region is proposed based on changes in chemical shift between the free and interacting species. The changes in ^{1}H and ^{15}N for each residue were plotted in two dimensions, and an elliptical cutoff was used (as in [12]) to determine which residues were significantly shifted. These residues are labeled in Fig. 2A, and their positions in the sequence are highlighted in Fig. 4. With the exception of four residues in subdomain 3 close to the hinge region between N- and C-terminal domains, all of the residues are located in subdomain 5 (nomenclature from Stallings et al. [5]). Residues 165, 168, and 192–197 are located in loop regions between the β-sheet and α-helix segments of this subdomain. Some of these may be directly involved in binding, resulting in positional shifts in adjacent and nearby residues. The other residues in subdomain 5 whose chemical shifts change, are located in secondary structural elements which are connected to the loop regions just mentioned, and these changes can be explained by induced structural adjustments in hydrogen bonding networks. Only four residues in subdomain 3 change their chemical shifts: 23, 26, 27, and 50. The first three of these are located in helix 3b, which is on the surface of the interdomain interface and has been implicated in S3P binding by deuterium exchange experiments [9].

3.2. Secondary structure comparison

The secondary structure prediction methods outlined by Wishart et al. [13] and Wüthrich et al. [14] were employed for the liganded N-terminal domain. Both methods predict that the isolated domain retains its native structure. The chemical shift index (CSI) of the N-terminal domain plus S3P predicts most of the same structural elements, with the exception of the C-terminal β-strand (Fig. 3). Also in the S3P-bound state, there are several additional NOEs observed in residues 154–160 (Fig. 4), the segment linking subdomains 4 and 5.

4. Discussion

Based on their location on the inner face of the N-terminal domain, which comprises half of the active site, residues identified in this study that may be involved in binding are Ser23, Arg27, Ser197, and Tyr200 (see Fig. 2B). The behavior of Tyr200 is especially interesting: as titration with S3P proceeds, its peak visibly broadens, presumably due to chemical exchange, and shifts by small degrees from its original position to its S3P-bound position. This residue is mentioned in [6,7] as one that undergoes a major conformational change upon S3P binding. Ser23 and Arg27 have been subjected to

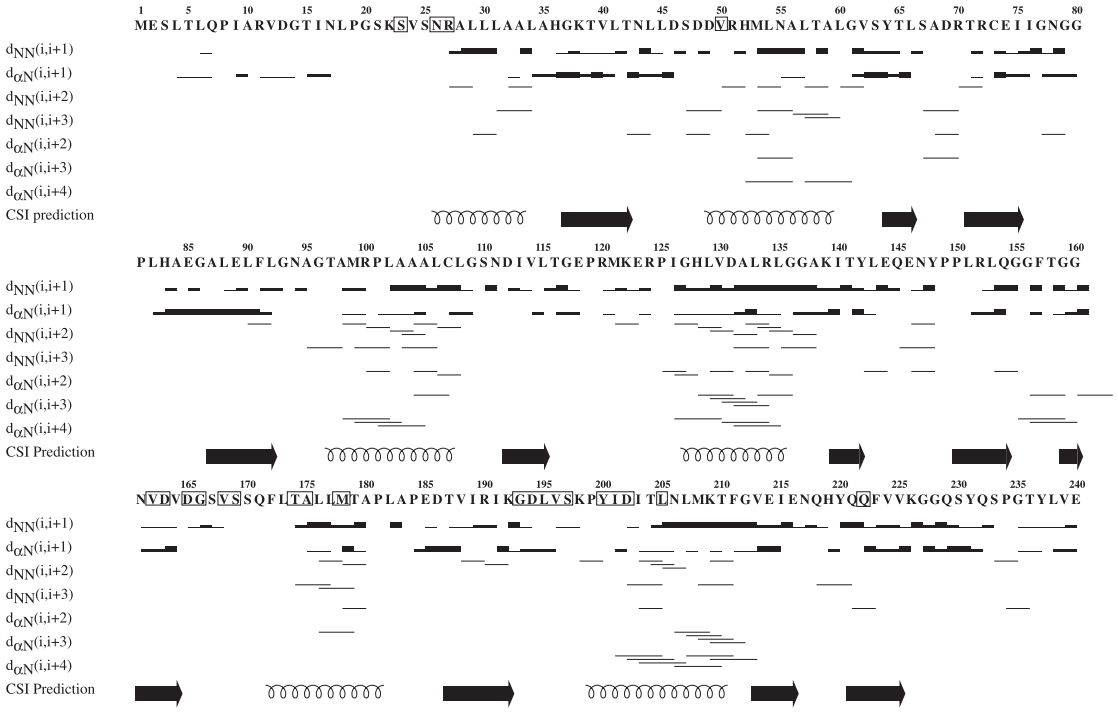

Fig. 4. A summary of the NOE data defining the secondary structure of the N-terminal domain in the presence of S3P. For the sequential NOEs involving H^N and H^α protons, the NOE intensities are indicated by the width of the bars. The bottom line of each panel shows the secondary structure predicted by CSI for comparison. Residue labels outlined in boxes are those whose chemical shifts change significantly upon binding to S3P.

mutagenesis (unpublished results and [15]), with 10% and undetectable residual activity, respectively, for the alanine substitutions. Ser23 is involved in S3P binding only in the Schönbrunn binary complex structure [7], while Arg27 and Ser197 are implicated in both binary complex structures. Ser197 makes one hydrogen bond to S3P in the closed structure [7], but two in the open structure [6]. It will be important to define the roles of these residues in the solution state structure for an accurate understanding of S3P binding.

While the CSI and NOE graphs predict that the basic secondary structural elements of the N-terminal domain do not change upon either isolation or S3P binding, there are some subtle but distinct differences observed between the free and S3P-bound states. First, the CSI predicts a shortened β-strand at residue 140 based on the chemical shifts of the S3P-bound species. The pattern of long-range NOEs is also different in this region: $^1H^N$–$^1H^\alpha$ correlations are lost between Q154 and I140 and gained between T141 and L151. Secondly, there are five additional NOEs observed for the S3P-bound species (all medium range and of the type $^1H^N$–$^1H^\alpha$) in the segment 154–160, which links subdomains 4 and 5. This means that the last two secondary structural elements of subdomain 4 are required to undergo some structural reorganization upon binding to S3P. This is an interesting point, since the linking segment is at a maximal distance from the active site cleft. Clearly, though the substrate binding is localized, the structural rearrangements it induces are not.

From these results, we propose a partial conformational change in which subdomain 4 shifts with respect to subdomain 5 upon S3P binding. A partial conformational change upon S3P binding is supported by the results of Stepanek [16], who found that monoclonal antibodies could be raised against the binary EPSPS•S3P complex, distinct from antibodies that recognized the enzyme alone. Also, Krekel et al. [17] found that S3P binding did not increase the dissociation constant of a monoclonal antibody raised against EPSP synthase, implying that S3P alone did not induce a full conformational change that disrupted the recognition of the antibody. This contrasted with the results of their mass spectrometric analysis, and could be explained by hypothesizing that S3P induced only a partial conformational change that allowed the antibody access to its epitope while restricting the access of trypsin to proteolytic cleavage sites. Our NMR data support this hypothesis and serve to describe the nature of the partial conformational change as it occurs in the N-terminal domain.

It is clear from the ternary enzyme•S3P•GLP structure [7] that residues from both domains contribute to the active site of EPSP synthase. One remaining question regarding the formation of the active site is whether or not S3P alone triggers the shift to a closed conformation. The isolation of the domains of EPSP synthase, originally designed to facilitate the NMR assignment process, has provided a means of answering this question by deconvolution of the contributions of the individual domain to the events of binding and catalysis. For instance, we showed previously that the N-terminal domain is the primary energetic contributor to S3P binding [9], which suggests the possibility of an open binary complex and lends support to the Stallings structure [6]. Furthermore, the isolation of the N-terminal domain will eventually allow the differentiation of the effects of S3P binding and domain closure from comparison of the solution state structure with the closed binary crystal structure.

In summary, chemical shift mapping localizes S3P binding to selected residues in subdomains 3 and 5, a limited number of which are logical candidates for substrate binding based on their position at the active site. Secondary chemical shift and

NOE data indicate that a majority of the secondary structural elements present in the protein fragment alone are undisturbed by substrate binding. Exceptions to this finding suggest a relative conformational shift of subdomains 4 and 5 upon S3P binding. Our results agree well with, and help to explain, previous biochemical and structural studies. They will provide the basis for further NMR studies on the structural and functional properties of EPSP synthase.

Acknowledgements: This research was supported by NIH grant R01 GM43215. The WSU NMR Center equipment was supported by NIH grants RR0631401 and RR12948, NSF grants CHE-9115282 and DBI-9604689, and a grant from the Murdock Charitable Trust. We thank Linda K. Nicholson and Theresa A. Ramelot for sending us the CSI and NOE data plotting programs, and for advising us on how to use them.

References

[1] Du, W., Wallis, N.G., Mazzulla, M.J., Chalker, A.F., Zhang, L., Liu, W.S., Kallender, H. and Payne, D.J. (2000) Eur. J. Biochem. 267, 222–227.
[2] Roberts, F., Roberts, C.W., Johnson, J.J., Kyle, D.E., Krell, T., Coggins, J.R., Coombs, G.H., Milhous, W.K., Tzipori, S., Ferguson, D.J.P., Chakrabarti, D. and McLeod, R. (1998) Nature 393, 801–805.
[3] Kishore, G.M. and Shah, D.M. (1988) Annu. Rev. Biochem. 57, 627–663.
[4] Steinrucken, H.C. and Amrhein, N. (1984) Eur. J. Biochem. 143, 351–357.
[5] Stallings, W.C., Abdelmeguid, S.S., Lim, L.W., Shieh, H.S., Dayringer, H.E., Leimgruber, N.K., Stegeman, R.A., Anderson, K.S., Sikorski, J.A., Padgette, S.R. and Kishore, G.M. (1991) Proc. Natl. Acad. Sci. USA 88, 5046–5050.
[6] Franz, J.E., Mao, M.K. and Sikorski, J.A. (1997) in: Glyphosate: A Unique Global Herbicide, ACS Monograph 189, pp. 546–550, American Chemical Society, Washington, DC.
[7] Schönbrunn, E., Eschenburg, S., Shuttleworth, W.A., Schloss, J.V., Amrhein, N., Evans, J.N.S. and Kabsch, W. (2001) Proc. Natl. Acad. Sci. USA 98, 1376–1380.
[8] Stauffer, M.E., Young, J.K., Helms, G.L. and Evans, J.N.S. (2001) J. Biomol. NMR, in press.
[9] Stauffer, M.E., Young, J.K. and Evans, J.N.S. (2001) Biochemistry 40, 3951–3957.
[10] Meininger, D.P., Rance, M., Starovasnik, M.A., Fairbrother, W.J. and Skelton, N.J. (2000) Biochemistry 39, 26–36.
[11] Bergkvist, A., Johansson, C., Johansson, T., Rydstrom, J. and Karlsson, B.G. (2000) Biochemistry 39, 12595–12605.
[12] Wang, Y.-X., Neamati, N., Jacob, J., Palmer, I., Stahl, S.J., Kaufman, J.D., Huang, P.L., Huang, P.L., Winslow, H.E., Pommier, Y., Wingfield, P.T., Lee-Huang, S., Bax, A. and Torchia, D.A. (1999) Cell 99, 433–442.
[13] Wishart, D.S., Sykes, B.D. and Richards, F.M. (1992) Biochemistry 31, 1647–1651.
[14] Wüthrich, K., Billeter, M. and Braun, W. (1984) J. Mol. Biol. 180, 715–740.
[15] Shuttleworth, W.A., Pohl, M.E., Helms, G.L., Jakeman, D.L. and Evans, J.N.S. (1999) Biochemistry 38, 296–302.
[16] Stepanek, F. (1990) Ph.D. Thesis, Ruhr-Universität, Bochum.
[17] Krekel, F., Oecking, C., Amrhein, N. and Macheroux, P. (1999) Biochemistry 38, 8864–8878.